JCB Journal of Cell Biology

ARTICLE

Pancreatic tumor cell metastasis is restricted by MT1-MMP binding protein MTCBP-1

Li Qiang[1], Hong Cao[3], Jing Chen[3], Shaun G. Weller[3], Eugene W. Krueger[3], Lizhi Zhang[4], Gina L. Razidlo[2,3], and Mark A. McNiven[2,3]

The process by which tumor cells mechanically invade through surrounding stroma into peripheral tissues is an essential component of metastatic dissemination. The directed recruitment of the metalloproteinase MT1-MMP to invadopodia plays a critical role in this invasive process. Here, we provide mechanistic insight into MT1-MMP cytoplasmic tail binding protein 1 (MTCBP-1) with respect to invadopodia formation, matrix remodeling, and invasion by pancreatic tumor cells. MTCBP-1 localizes to invadopodia and interacts with MT1-MMP. We find that this interaction displaces MT1-MMP from invadopodia, thereby attenuating their number and function and reducing the capacity of tumor cells to degrade matrix. Further, we observe an inverse correlation between MTCBP-1 and MT1-MMP expression both in cultured cell lines and human pancreatic tumors. Consistently, MTCBP-1–expressing cells show decreased ability to invade in vitro and metastasize in vivo. These findings implicate MTCBP-1 as an inhibitor of the metastatic process.

Introduction

Pancreatic ductal adenocarcinoma (PDAC) is an exceptionally lethal cancer, in part due to its aggressive invasiveness and metastatic properties. Unfortunately, the current anti-tumor drugs used to treat this cancer are toxic and largely ineffective (American Cancer Society, 2015, 2017; Siegel et al., 2016, 2017). Thus, understanding the underlying mechanism of PDAC invasion and metastatic dissemination is key to the development of new therapies.

Metastatic tumors are known to actively remodel the surrounding extracellular matrix (ECM) to facilitate invasion into nearby organs and vessels (Ridley, 2011). One stromal remodeling mechanism used by tumor cells is the formation of invadopodia, actin-rich membrane protrusions that extend from the cell surface into the surrounding ECM (Murphy and Courtneidge, 2011; Eddy et al., 2017). These structures are composed of numerous cytoskeletal proteins, kinases, and phosphatases, as well as large and small GTPases (Gimona et al., 2008; Chan et al., 2009; Murphy and Courtneidge, 2011; Ridley, 2011; Paterson and Courtneidge, 2018) that act to deform the cell membrane while also recruiting matrix metalloproteinases (MMPs; Artym et al., 2006; Clark et al., 2007; Poincloux et al., 2009). Among the many MMPs expressed in cells, MT1-MMP is believed to be the most relevant for invadopodia function, although its regulation at invadopodia is still not well understood (Sabeh et al., 2009; Jacob and Prekeris, 2015). MT1-MMP has been studied extensively and has an extracellular catalytic domain, a single transmembrane domain, and a short, 20–amino acid cytoplasmic tail (CT; Rahib et al., 2014). This tail is believed to bind to actin filaments within the invadopodia to facilitate its recruitment and retention (Yu and Machesky, 2012; Yu et al., 2012). The fact that MT1-MMP is overexpressed in many tumor types and is key to stromal remodeling has made it an attractive therapeutic target, although clinical trials implementing chemical inhibitors have had limited success, due in part to nonspecific targeting of other MMPs (Egeblad and Werb, 2002; Rakash, 2012; Pahwa et al., 2014). Defining the role of cellular proteins that bind and modulate this important protease is likely to provide new insights into understanding its function and regulation and providing more targeted therapies.

Membrane-type 1 matrix metalloproteinase CT binding protein-1 (MTCBP-1) is an understudied protein that has been demonstrated to bind to the CT of MT1-MMP and reduce MT1-MMP–dependent migration in fibrosarcoma cells in vitro (Uekita et al., 2004). Whether this interaction might alter stromal remodeling by tumor cells or metastasis is unclear. Further, the mechanisms by which MTCBP-1 might attenuate MT1-MMP–dependent processes are unknown.

In this study, our goal was to define the role for MTCBP-1 in PDAC metastasis. We have observed that MTCBP-1 is targeted to invadopodia where it significantly reduces the capacity of PDAC

[1]Biochemistry and Molecular Biology Program, Mayo Clinic Graduate School of Biomedical Sciences, Mayo Clinic, Rochester, MN; [2]Department of Biochemistry and Molecular Biology, Mayo Clinic, Rochester, MN; [3]Center for Basic Research in Digestive Diseases, Division of Gastroenterology and Hepatology, Mayo Clinic, Rochester, MN; [4]Department of Laboratory Medicine, Mayo Clinic, Rochester, MN.

Correspondence to Mark A. McNiven: mmcniven@mayo.edu.

cells to accumulate these functional degradative structures. As a result, the capacity of MTCBP-1–expressing tumor cells to degrade the surrounding substrate and subsequently invade through transwell migration chambers in vitro is markedly impaired. Accordingly, the ability of MTCBP-1–expressing cancer cells to metastasize into peripheral tissues is also substantially decreased. We provide mechanistic insights into these physiological outcomes through the identification of a region within the CT of MT1-MMP to which MTCBP-1 binds. This interaction is used for targeting MTCBP-1 to invadopodia while reducing the interaction of MT1-MMP with the invadopodial actin scaffold. These findings provide new insights into invadopodia biology and support the premise of MTCBP-1 as an endogenous antimetastatic factor in tumor cells.

Results

MTCBP-1 attenuates the invasive properties of tumor cells and associates with invadopodia

As MTCBP-1 interacts with MT1-MMP (Uekita et al., 2004), a known driver of ECM degradation and tumor cell invasion, we tested if expression of MTCBP-1 impacts the capacity of PDAC cells to invade in vitro. To this end, PDAC cells were seeded in a chemotactic transwell invasion assay following siRNA-mediated knockdown of MTCBP-1. Cells depleted of MTCBP-1 exhibited significantly more invasion than did the control cells treated with a nontargeting siRNA (Fig. 1, A and B; and Fig. S1, A–C). These findings are consistent with those previously observed in fibrosarcoma cells, where overexpression of MTCBP-1 decreased the transwell invasion ability of HT1080 cells, suggesting that MTCBP-1 potentially suppresses tumor cell invasion in vitro (Uekita et al., 2004).

The remodeling of the ECM by invadopodia and related structures is essential for tumor cell dissemination and invasion. Because MTCBP-1 interacts with the invadopodial component MT1-MMP, we predicted that loss of MTCBP-1 might modify the ability to degrade the surrounding substrate. We quantified both the percentage of cells capable of degrading a fluorescent gelatin matrix, as well as the area of degradation per cell. Importantly, loss of MTCBP-1 significantly increased the degradation of the ECM. Silencing of MTCBP-1 resulted in a fourfold increase in the degradation area/cell area in DanG cells and a twofold increase in the degradation area/cell area in BxPC3 cells. The percentage of cells capable of degrading the matrix was increased by twofold in the absence of MTCBP-1 in BxPC3 cells. This change is minimal in DanG cells since >90% of DanG cells were capable of degrading the matrix in the control group under this condition (Fig. 1, C and D; and Fig. S1, D and E). Strikingly, Panc-1 cells, which are normally unable to degrade substrates due to low MT1-MMP levels, exhibited a 19-fold increase in the percentage of cells capable of degrading gelatin following MTCBP-1 knockdown (Fig. 1 E and Fig. S1 F). The overall total cell area remained unchanged upon manipulation of MTCBP-1 protein levels (Fig. S2, A–D). The findings that the loss of MTCBP-1 increased matrix degradation and transwell invasion suggest that MTCBP-1 suppresses the capacity of these tumor cells to remodel the surrounding matrix.

As a reciprocal approach to the knockdown experiments, we tested whether cells overexpressing MTCBP-1 exhibited reduced invasive capacity. To this end, several stable cell lines (Panc1, BxPC3, and DanG) were generated to overexpress either MTCBP-1-FLAG or FLAG control vector and plated in transwell invasion assays as described above. As shown in Fig. 2 (A–C), overexpression of MTCBP-1 reduced transwell migration by >50%.

Because of this reduced invasive capacity, the MTCBP-1-FLAG–expressing cells (DanG) were tested for matrix degradation by plating on fluorescent gelatin as described in Fig. 1. Importantly, the number of the MTCBP-1–expressing cells exhibiting gelatin degradation was reduced by 17%, while the area of degradation was decreased by threefold (Fig. 2 D) and the cell area remained constant (Fig. S2 D). These data are consistent with those presented in Fig. 1 (C–E) and indicate that MTCBP-1 can inhibit the matrix-degrading and invasive potential of tumor cells.

To confirm that inhibition of MT1-MMP was the central factor in the observed increase in metastatic potential of the MTCBP-1 knockdown cells, Panc-1, BxPC3, and DanG cells were treated with siRNAs against MT1-MMP and tested for matrix degradation and cell invasion. Importantly, these properties were markedly attenuated in these double knockdown cells, indicating the inhibitory effect of MTCBP-1 is dependent on the presence of MT1-MMP (Fig. S1, A–F).

As the actin-rich invadopodia at the cell base are the primary site for matrix remodeling during invasion, we tested if MTCBP-1 inhibited invadopodia formation or function. As displayed in Fig. 2 (E and F), DanG or BxPC3 cells stably overexpressing MTCBP-1-FLAG exhibited only 20–30% as many Tks5-positive invadopodia compared with control cells. This reduced number of invadopodia coupled with attenuated matrix degradation in MTCBP-1–expressing cells (Fig. 2 D) suggested that this protein may be playing an inhibitory role directly at the invadopodia, perhaps by altering the assembly, turnover, and/or function of these invasive structures. To test this premise, BxPC3 cells stably overexpressing FLAG or MTCBP-1-FLAG were transfected with Tks5-GFP constructs and subjected to live-cell imaging on gelatin-coated imaging dishes for 16 h and 40 min at 5 min intervals. Indeed, the average invadopodial lifetime in BxPC3 cells stably overexpressing MTCBP-1-FLAG was substantially reduced ∼50% compared with control cells (Fig. S2, E and F; and Videos 1 and 2), suggesting that invadopodia become more transient in cells expressing increased levels of MTCBP-1.

MTCBP-1 inhibits matrix degradation through a direct interaction with MT1-MMP

MTCBP-1 is known to bind to the 20–amino acid CT of MT1-MMP (Uekita et al., 2004), although the specific domains within either of these proteins that mediate this interaction are undefined. To identify these interactive regions, MT1-MMP-GFP was overexpressed in DanG cells that were then homogenized and subjected to co-immunoprecipitation (co-IP) with an MTCBP-1 antibody. Indeed, MT1-MMP was able to co-precipitate with MTCBP-1, suggesting the two proteins associate in cells (Fig. 3 A). The interaction between the endogenous MTCBP-1 and the CT domain of MT1-MMP protein (MT1-CT) was further confirmed by using purified GST-MT1-CT to pull down MTCBP-1 from lysates from

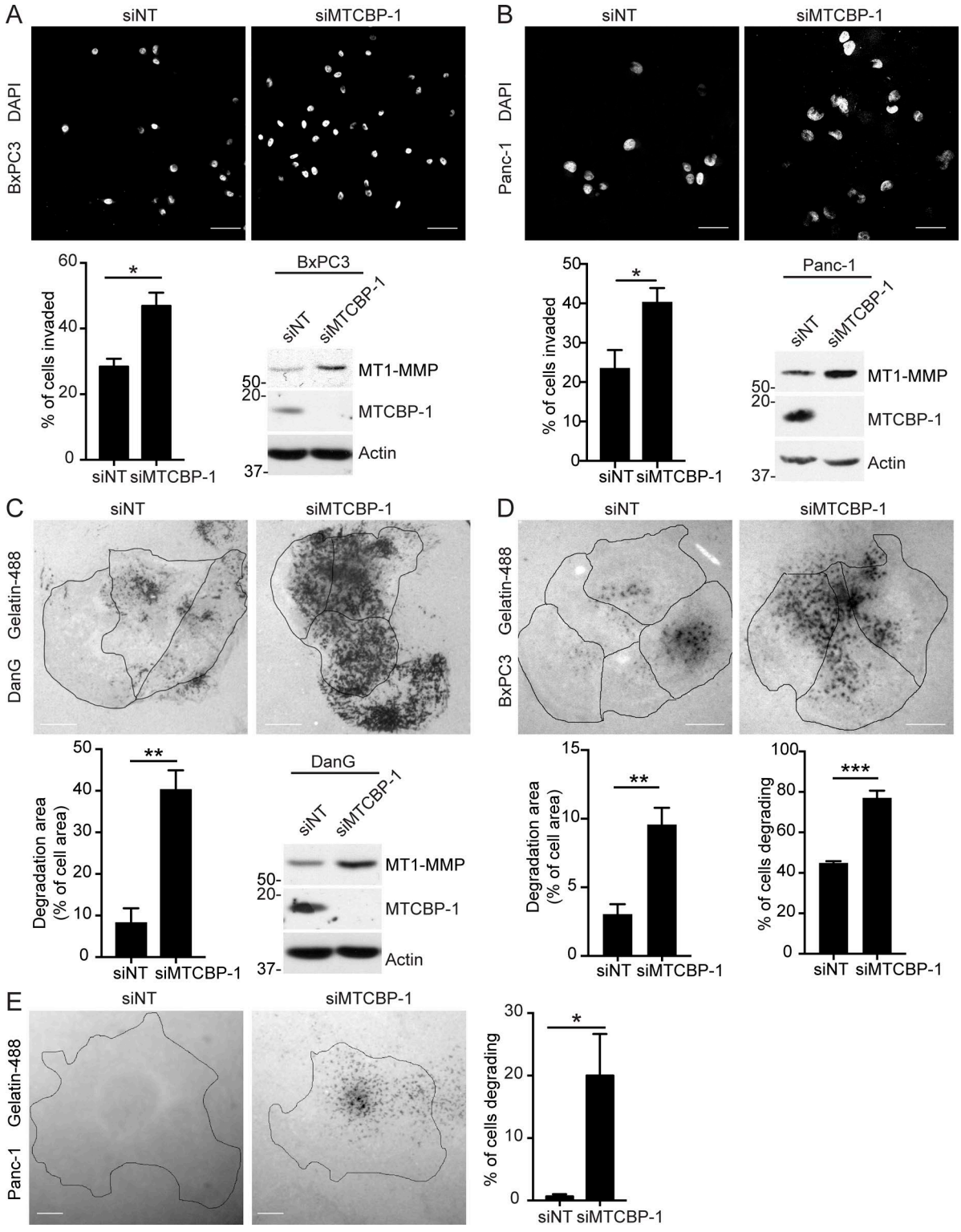

Figure 1. **Depletion of MTCBP-1 promotes the invasive properties of pancreatic cancer cells. (A and B)** Loss of MTCBP-1 increases invasive migration of PDAC cells. BxPC3 cells (A) or Panc-1 cells (B) were transfected with control or siRNA against MTCBP-1 for 2 d and then seeded in a transwell invasion assay for 6 h (BxPC3) or 24 h (Panc-1). The percentage of cells that invaded across the filter was counted by DAPI staining after fixation. The knockdowns were confirmed by Western blot. Graphs represent normalized averages ± SEM from three independent experiments. *, P < 0.05. Bars, 50 µm. **(C–E)** MTCBP-1 depletion promotes ECM degradation by PDAC cells. DanG cells (C), BxPC3 cells (D), and Panc-1 cells (E) were treated with control or siRNA targeting MTCBP-1 for 2 d and then seeded onto green fluorescent gelatin-coated coverslips. Gelatin degradation was quantified after 8 h (DanG), 6 h (BxPC3), or 24 h (Panc-1). Bars: 20 µm (C); 20 µm (D); 10 µm (E). Reduction of MTCBP-1 results in a 2–19-fold increase in the percentage of cells degrading the gelatin substrate in BxPC3 and Panc-1 cells (≥100 cells per condition) and a 3–5 fold increase in the area degraded per cell in BxPC3, DanG, and Panc-1 cells (≥10 cells per condition). The results represent the mean ± SEM of three independent experiments. *, P < 0.05; **P < 0.005; ***, P < 0.0005. The knockdown efficiency was confirmed by Western blot. All blot measurements in kD.

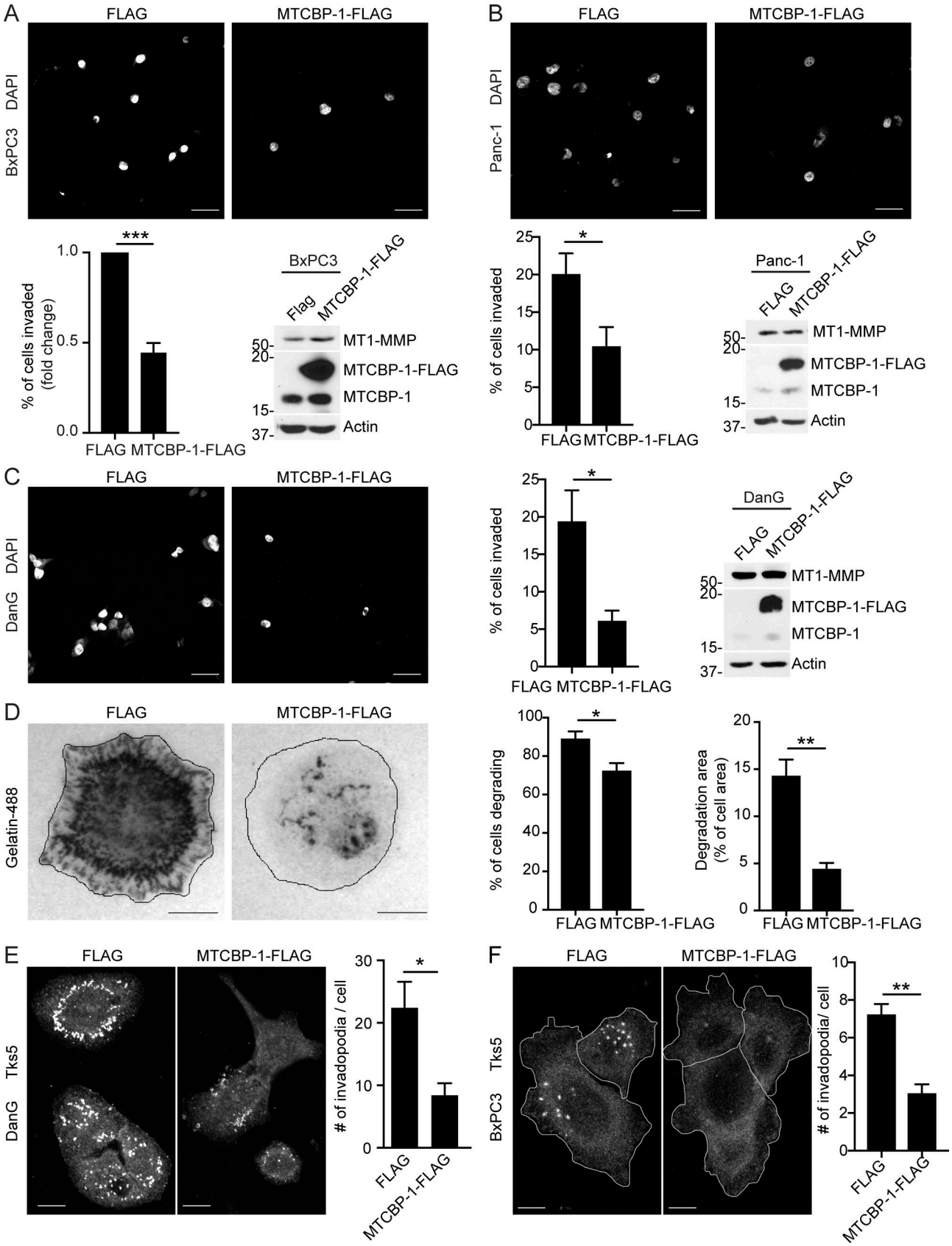

Figure 2. **MTCBP-1 overexpression inhibits the invasive properties of pancreatic cancer cells. (A–C)** MTCBP-1 overexpression inhibits transwell invasion of PDAC cells. BxPC3 cells (A), Panc-1 cells (B), or DanG cells (C) stably expressing FLAG control or MTCBP-1-FLAG were seeded in transwell invasion assays for 6 (BxPC3), 24 (Panc-1), or 48 h (DanG) and counted by DAPI staining after fixation. A more than threefold reduction in the number of cells migrating through the filters was observed in MTCBP-1–expressing cells. The stable overexpression was confirmed by Western blot. Bars, 50 µm. **(D)** MTCBP-1 overexpression

DanG cells (Fig. 3 B). To confirm these interactions are direct, a far-Western overlay binding assay was performed using purified His-tagged MTCBP-1 as a probe. Consistent with the IP and GST pulldown experiments, GST-MT1-CT, but not GST alone, interacts with purified MTCBP-1 directly (Fig. 3 C). Together, these data confirm a direct interaction between MTCBP-1 and the CT of MT1-MMP.

To define the specific regions that mediate the interaction between MT1-MMP and MTCBP-1, we again used a far-Western blotting approach using different GST-MT1-CT truncations (Fig. 3 D). While binding was observed between both full-length proteins, the interaction was abolished when deleting the 10 amino acids at the N terminus of MT1-CT (GST-C-10), while a truncation of the 10 amino acids at the C terminus of MT1-CT (GST-N-10) does not reduce the interaction (Fig. 3 E). Further deletion analysis of the interacting N-terminal region of the cytoplasmic MT1-MMP tail suggests that a 3–amino acid region (PRR) mediates the binding between MTCBP-1 and MT1-MMP (Fig. 3 F). Deletion of PRR$^{568–570}$ on MT1-MMP abolished the interaction with MTCBP-1.

To address if the direct interaction between MT1-MMP and MTCBP-1 is critical for the inhibitory role of MTCBP-1 in PDAC invasion, a full-length MT1-MMP construct missing residues PRR$^{568–570}$ (MT1-MMP-ΔPRR-mCherry) was expressed in cells and compared with WT MT1-MMP-mCherry. Panc-1 cells are normally incapable of degrading gelatin matrix due to very low levels of endogenous MT1-MMP, while exogenous overexpression of MT1-MMP induces extensive matrix degradation (Fig. 3 G, a and c; Wang and McNiven, 2012). This robust MT1-MMP–dependent matrix degradation was nearly abolished by the overexpression of MTCBP-1-FLAG (Fig. 3 G, d). MT1-MMP-ΔPRR was equally capable of inducing robust matrix degradation (Fig. 3 G, e). Importantly, MTCBP-1-FLAG was no longer able to suppress matrix degradation in cells expressing MT1-MMP-ΔPRR, which cannot interact with MTCBP-1 (Fig. 3 G, f). These data indicate that MTCBP-1 suppresses invasive matrix degradation through its interaction with MT1-MMP.

As the actin-rich invadopodia at the cell base are the primary sites for matrix remodeling during invasion (Linder, 2007; McNiven, 2013), it was important to test if MTCBP-1 might reside at these structures. To test this, BxPC3 cells stably expressing MTCBP-1-FLAG were seeded on green fluorescent gelatin-coated coverslips. Strikingly, these cells show a colocalization of MTCBP-1 with actin structures and sites of matrix degradation, which represent conventional invadopodia (Fig. 4 A). Moreover, confocal orthogonal views also show MTCBP-1-FLAG localized at the protrusive invadopodial structures at sites of substrate degradation (Fig. 4 B). These data identify a novel localization of MTCBP-1 to invadopodia, which we propose is related to its inhibition of invadopodia-mediated matrix degradation.

Based on the findings in this manuscript (Fig. 3, A–F) and others (Uekita et al., 2004) that MTCBP-1 is a MT1-MMP binding protein, we hypothesized that these proteins might be colocalized at invadopodia. To test this question, BxPC3 cells stably expressing MTCBP-1-FLAG were seeded on gelatin-coated coverslips. Imaging of these cells showed a consistent colocalization between MTCBP-1-FLAG and endogenous MT1-MMP at several, but not all, degradation sites (Fig. S3 A). No colocalization was observed at other cellular locations, suggesting that invadopodia may be the primary site of MTCBP-1 function. To address if the direct interaction between MT1-MMP and MTCBP-1 is critical for the localization of MTCBP-1 at invadopodia, BxPC3 cells stably expressing MTCBP-1-FLAG were treated with siRNA against MT1-MMP, followed by reexpression of WT MT1-MMP-mCherry, MT1-MMP-ΔPRR-mCherry incapable of binding with MTCBP-1, or a control mCherry vector (Fig. S3 B). The data indicate that MTCBP-1 could colocalize with Tks5-positive invadopodia in cells expressing either WT MT1-MMP or MT1-MMP-ΔPRR. This result indicates that the localization of MTCBP-1 at invadopodia is independent of binding to MT1-MMP; however, the recruiting mechanism of MTCBP-1 at invadopodia is unclear.

Based on the binding and localization studies displayed in Fig. 3 and Fig. 4, we next asked if the targeted accumulation of MT1-MMP to invadopodia might be diminished by increasing MTCBP-1 expression. To test this, DanG cells stably expressing FLAG or MTCBP-1-FLAG were seeded on gelatin-coated coverslips for 8 h. Following fixation these cells were viewed and the number of actin-positive invadopodial structures with or without associated MT1-MMP were counted. A substantial reduction (50%) in the number of MT1-MMP–positive invadopodia in MTCBP-1-FLAG overexpressing cells was observed (Fig. S3 C). A similar trend in another pancreatic cell line (BxPC3) was also observed using a second invadopodial marker, Tks5 (Fig. S3 D). These data suggest that MTCBP-1 may inhibit the accumulation of MT1-MMP to invadopodia, leading to decreased stromal remodeling, perhaps by reducing the recruitment or the retention of MT1-MMP.

MTCBP-1 disrupts the interactions between MT1-MMP and F-actin

An important finding by Machesky et al. (Yu et al., 2012) described a LLY region in the CT of MT1-MMP (residue 571–573) that mediates the interaction of the protease with actin filaments and is essential for targeting to invadopodia, efficient matrix remodeling, and invasive migration. Importantly, this domain is directly adjacent to the MTCBP-1–binding PRR region that we have just identified (PRR$^{568–570}$; Fig. 3). Thus, it was attractive to predict that MTCBP-1 might reduce invadopodia formation and function by competing with the actin-binding site on the CT of

suppresses the ECM degradation of PDAC cells. DanG cells stably expressing FLAG control or MTCBP-1-FLAG were seeded on green fluorescent gelatin-coated coverslips and matrix degradation was quantified after 8 h. MTCBP-1 overexpression led to a reduction in the number of cells degrading matrix as well as the area of degradation per cell. Graphs represent normalized averages ± SEM from three independent experiments. Bars, 10 µm. **(E and F)** MTCBP-1 overexpression reduces invadopodia number in PDAC cells. DanG (E) or BxPC3 (F) cells stably expressing FLAG or MTCBP-1-FLAG were seeded on gelatin-coated coverslips and stained for Tks5 to mark invadopodia. MTCBP-1 overexpression reduces the number of Tks5-positive invadopodia in DanG and BxPC3 cells comparing to the controls. Graphs represent normalized averages ± SEM from three independent experiments. *, P < 0.05; **, P < 0.005; ***, P < 0.0005. Bars, 10 µm. All blot measurements in kD.

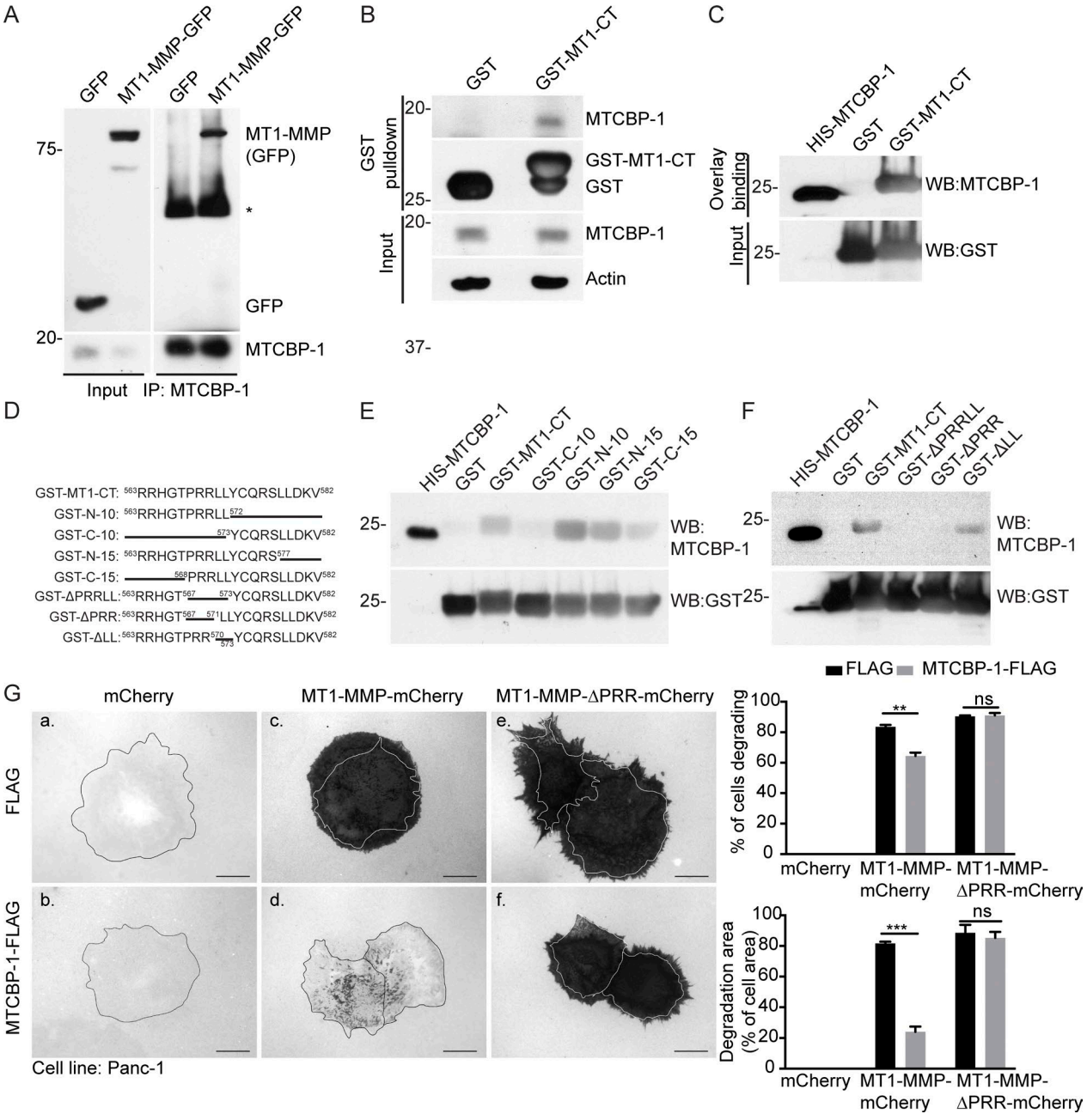

Figure 3. **MTCBP-1 binds the CT of MT1-MMP directly to inhibit the invasive properties of pancreatic cancer cells. (A)** DanG cells were transfected with GFP or MT1-MMP-GFP, and lysates were immunoprecipitated for MTCBP-1 and blotted for GFP. MT1-MMP-GFP co-immunoprecipitates with MTCBP-1. The asterisk indicates IgG. **(B)** The purified CT of MT1-MMP (GST-MT1-CT) was incubated with lysate from DanG cells. Endogenous MTCBP-1 co-precipitated with purified GST-MT1-CT, but not GST control. **(C)** A far-Western blot overlay binding assay was performed to test for a direct interaction between MTCBP-1 and MT1-MMP-CT. MTCBP-1 interacts directly with GST-MT1-CT, but not GST. **(D)** List of the GST fusion proteins used to map the domains on the CT domain of MT1-MMP that interact with MTCBP-1. **(E and F)** Far-Western blot overlays were performed to map the domains of direct interaction between MTCBP-1 and the CT domain of MT1-MMP protein (MT1-CT). Depletion of the 10 amino acids at the N terminus (GST-C-10) of MT1-CT abolishes the direct binding between MT1-CT and MTCBP-1. **(F)** Further analysis using additional truncation forms reveal that residues 568–570 (PRR), are key in mediating this interaction. **(G)** Functional analysis of the interaction between MT1-MMP and MTCBP-1. Panc-1 cells stably expressing FLAG or MTCBP-1-FLAG were transfected with mCherry control vector, MT1-MMP-mCherry, or MT1-MMP-ΔPRR-mCherry for 48 h and then seeded on green fluorescent gelatin-coated coverslips. Note that overexpression of MTCBP-1 inhibits gelatin degradation induced by MT1-MMP-mCherry, but not MT1-MMP-ΔPRR-mCherry, which cannot bind MTCBP-1. The graphs represent the mean ± SEM of the percentage of cells degrading the matrix ($n \geq 100$ cells per condition) or the area of gelatin degradation ($n \geq 10$ cells per condition) in three independent experiments. **, $P < 0.005$; ***, $P < 0.0005$; ns, not significant. Bars, 20 µm. All blot measurements in kD.

the MT-MMP. To test this, we first confirmed by co-IP that endogenous actin and MT1-MMP associate in PDAC cell homogenates (Fig. 5 A). Far-Western blot overlay experiments were performed to confirm that the purified MT1-MMP CT domain directly interacts with F-actin. GST protein alone was used as a negative control while the purified N terminus of α-Actinin

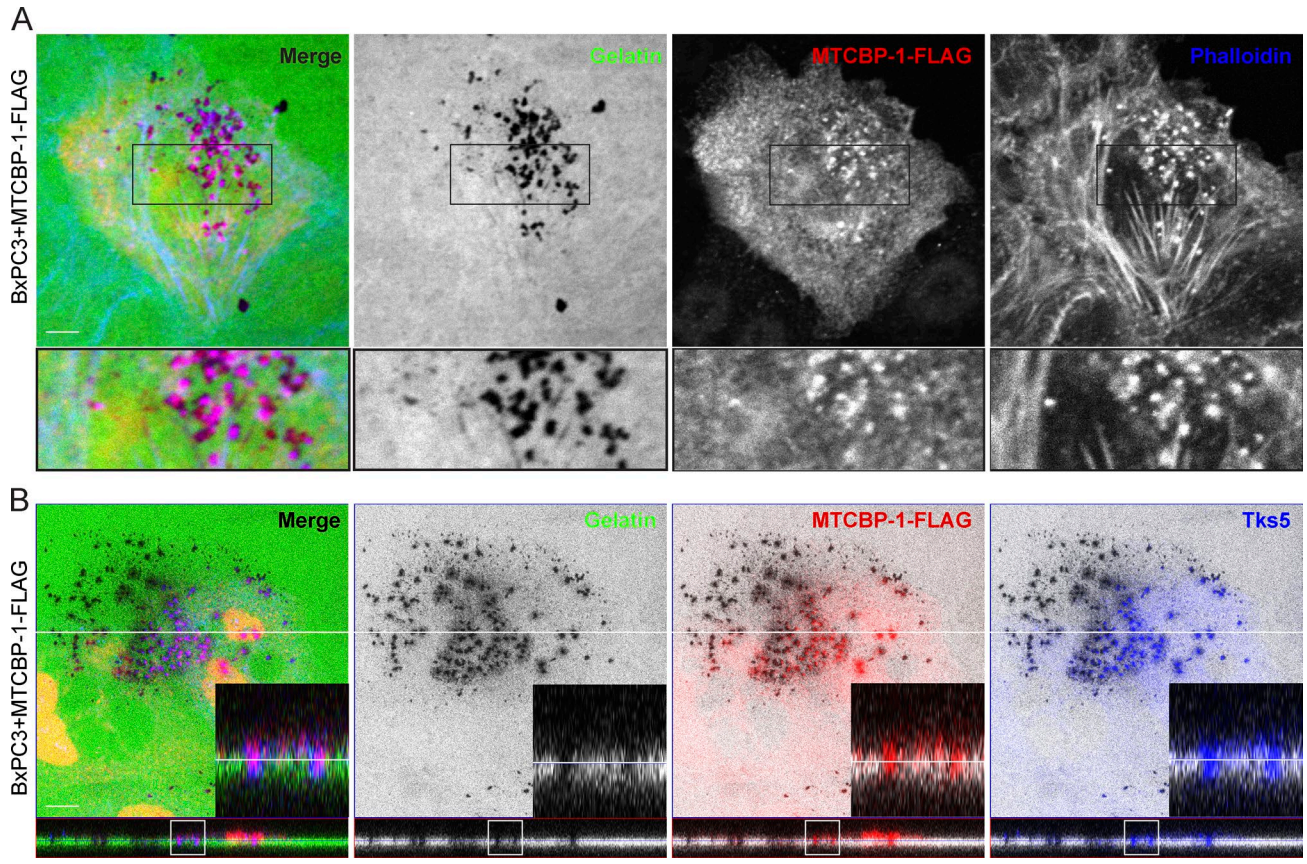

Figure 4. **MTCBP-1 resides at invadopodia in pancreatic cancer cells. (A and B)** BxPC3 cells stably expressing MTCBP-1-FLAG were seeded on green fluorescent gelatin-coated coverslips, and cells were either stained for FLAG and phalloidin (A) or the invadopodia marker Tks5 (B) to show the localization of MTCBP-1-FLAG at invadopodia. Transverse imaging of invadopodia is shown in B where both Tks5 and MTCBP-1 can be seen at sites of matrix loss. Boxed areas are magnified in insets. Bar, 10 µm.

(ACTN-N) was used as a positive control (Fig. 5 B). Indeed, F-actin directly bound to the CT of MT1-MMP (Fig. 5 B). Subsequently, modification of this assay allowed us to test if incubation of the immobilized proteins with MTCBP-1 disrupted the established association between MT1-MMP and F-actin. GST-MT1-CT was resolved on a gel and immobilized on a polyvinylidene fluoride (PVDF) membrane, again using GST as a negative control and GST-ACTN-N as a positive control. The membrane was probed with purified F-actin to allow binding between MT1-MMP-CT and actin, as in Fig. 5 B. Importantly, addition of purified MTCBP-1 to the filter-immobilized GST-proteins reduced the preestablished association between F-actin and GST-MT1-CT (Fig. 5 C). The amount of F-actin bound to GST-MT1-CT was significantly reduced following incubation with MTCBP-1. In contrast, MTCBP-1 had no effect on the association between the F-actin and the positive control GST-ACTN, suggesting that MTCBP-1 can specifically disrupt the binding between MT1-MMP-CT and F-actin (Fig. 5 C). This reduced association between MT1-MMP and actin is not a consequence of direct binding between MTCBP-1 and F-actin, as MTCBP-1 was not observed to bind to F-actin (Fig. 5 B). Collectively, these data suggest that MTCBP-1 disrupts the direct interaction between F-actin and the CT of MT1-MMP.

As an additional approach to overlay assays described above, actin co-sedimentation assays were also performed as described previously (Yu et al., 2012). We tested the capacity of increasing concentrations of the bacterially expressed HIS-MTCBP-1 to interfere with the binding of the GST-MT1-MMP CT to actin filaments, resulting in increasing amounts of the displaced protease in the supernatant. As displayed in Fig. 5 D, high levels of GST protein alone were observed in the supernatant, indicating no interaction with the actin pellet, and remained constant regardless of changing concentrations of MTCBP-1. Similarly, large amounts of the GST-tagged MT1-MMP CT were found in the supernatant in the absence of added F-actin, as predicted, but were markedly reduced in the supernatant upon the addition and pelleting of F-actin, consistent with actin binding (Fig. 5 E). Importantly, addition of HIS-MTCBP-1 to the reaction caused a dose-dependent increase of GST-MT1-CT in the supernatant, with a maximal effect observed at 5 µM HIS-MTCBP-1 (Fig. 5 F), consistent with release from F-actin. This saturable dose response to increasing HIS-MTCBP-1 concentrations supports the morphological (Fig. S3, C and D) and overlay experiments (Fig. 5 C), implicating MTCBP-1 in the disruption of MT1-MMP binding to invadopodial actin.

As we identified residues $PRR^{568-570}$ on the MT1-MMP CT as a key binding site for MTCBP-1 (Fig. 3, D–F), it was necessary to test if deletion of the PRR region would interfere with the binding between MT1-MMP and F-actin. Thus, Panc-1 cells were transfected to express control mCherry vector, WT MT1-MMP-mCherry, or

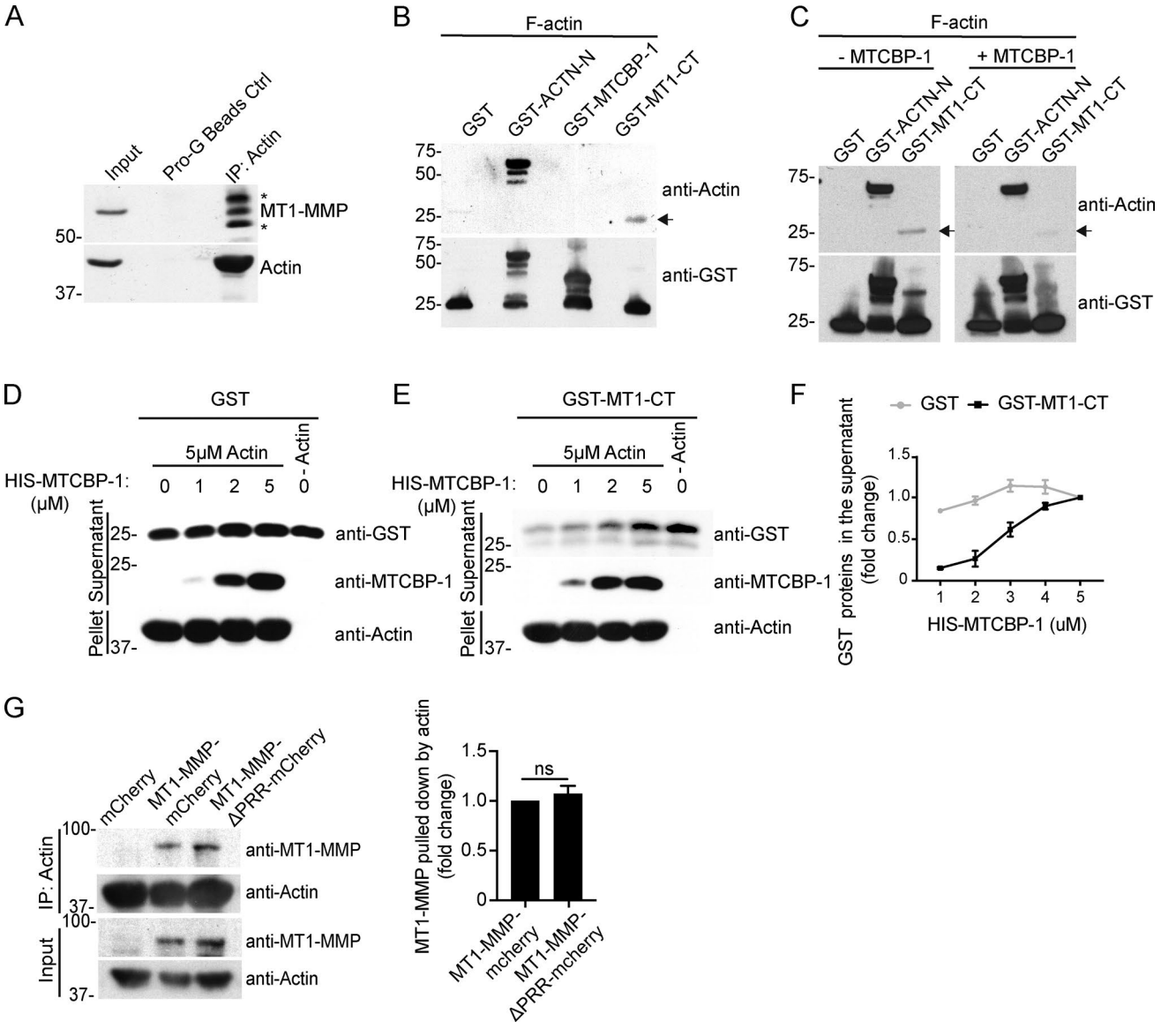

Figure 5. **MTCBP-1 disrupts the interactions between MT1-MMP and actin. (A)** DanG cell lysates were immunoprecipitated for actin and blotted for MT1-MMP, demonstrating an interaction between actin and MT1-MMP in PDAC cells. The asterisks indicate nonspecific bands. **(B)** Far-Western blot overlay indicates a direct binding between F-actin and MT1-MMP. GST and GST-ACTN-N were used as a negative control and a positive control, respectively. Actin associates with ACTN-N and MT1-MMP (arrow), but not MTCBP-1. **(C)** Modification of this overlay binding assay was used to test the role of MTCBP-1 in the association between MT1-MMP and F-actin. Addition of purified His-MTCBP-1 disrupts the preexisting association between F-actin and GST-MT1-CT, but not that between F-actin and GST-ACTN-N. **(D–F)** Actin co-sedimentation assays were performed to further define the role of MTCBP-1 in disrupting the association between MT1-MMP and F-actin. The interactions of GST or GST-MT1-CT with actin filaments was measured with an increasing amount of HIS-MTCBP-1. **(D)** MTCBP-1 does not affect the association between GST and F-actin. **(E)** Dose curve of HIS-MTCBP-1 demonstrating that HIS-MTCBP-1 displace GST-MT1-CT from the pellet to the supernatant in a dose-dependent manner from 1–5 μM. An increasing level of MT1-MMP is observed in the supernatant was observed. **(F)** Quantification of the co-sedimentation experiments detailed in D and E, reflecting an increase in the supernatant GST-MT1-CT levels, but not the supernatant GST levels after introducing an increasing amount of HIS-MTCBP-1. **(G)** Panc-1 cells were transfected with control mCherry, WT MT1-MMP-mCherry or MT1-ΔPRR-mCherry. Lysates were immunoprecipitated for actin and immunoblotted for MT1-MMP. Both WT and mutant MT1-MMP-ΔPRR bind to actin with equal intensity. Graphs shown in F and G represents normalized averages ± SEM from three independent experiments. ns, not significant. All blot measurements in kD.

MT1-ΔPRR-mCherry proteins, then subjected to lysis and IP with an antibody against actin (Fig. 5 G). As expected, MT1-MMP was co-immunoprecipitated with actin, and this interaction was not altered by deletion of PRR$^{568–570}$. The result shows that while MTCBP-1 can disrupt the interaction between MT1-MMP and F-actin, the binding sites for MTCBP-1 and F-actin on MT1-MMP are distinct. Collectively, these data indicate that MTCBP-1 inhibits the function of MT1-MMP at invadopodia by disrupting its association with F-actin (Fig. 8).

Metastatic invasion in vivo is markedly reduced in tumor cells expressing MTCBP-1

As MTCBP-1 overexpression attenuates the invasive properties of tumor cells in culture, it was important to test if these effects

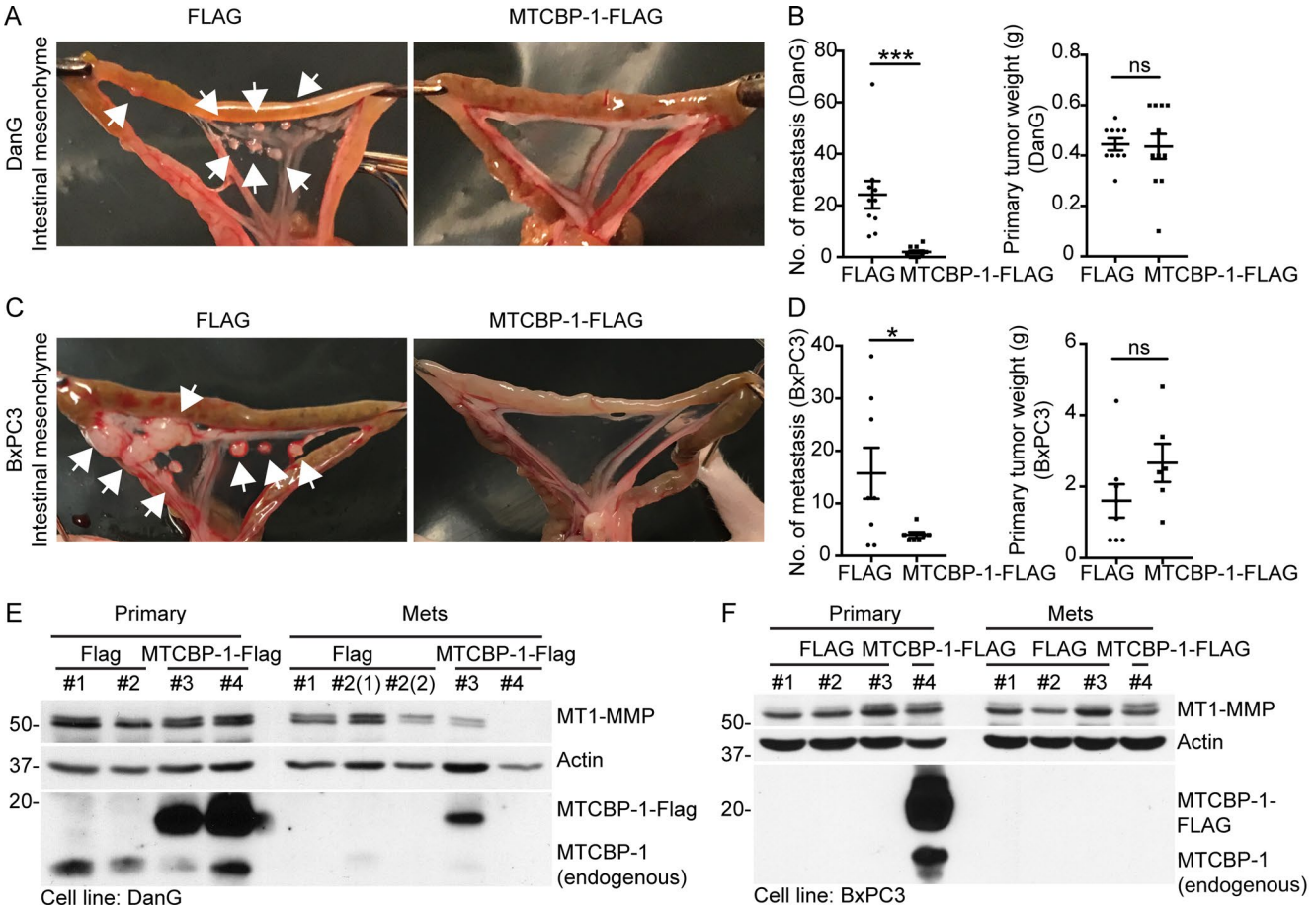

Figure 6. **MTCBP-1 overexpression significantly reduces metastasis of pancreatic cancer cells. (A and C)** Images of the small bowel of nude mice 18–20 d (DanG, A) or 8 wk (BxPC3, C) following orthotopic pancreatic injection of stable cell lines expressing either FLAG control or MTCBP-1-FLAG. The mice injected with control tumor cells formed a significant number of metastatic lesions (arrows) whereas metastasis was significantly reduced in the mice injected with MTCBP-1-FLAG–expressing tumor cells (A and C). **(B and D)** The number of macroscopic metastases and the primary tumor weight were scored upon necropsy. Graphs represent data from two independent experiments; lines represent averages ± SEM. *, $P < 0.05$; ***, $P < 0.0005$; ns, not significant. **(E and F)** Western blot demonstrating expression of MTCBP-1 and MT1-MMP in primary and metastatic tumors collected from mice that were orthotopically injected with virally transduced DanG cells (E) or BxPC3 cells (F). Note the decreased endogenous and ectopically expressed MTCBP-1 protein levels in metastases from mice #1, #2, #3, and #4 comparing to the corresponding primary tumor. Numbers at top of gel lanes (#1–4) represent individual mice. All blot measurements in kD.

translated to a reduction of metastatic potential in vivo. To address this, we used an orthotopic xenograft model with either highly invasive DanG or BxPC3 cell lines stably expressing MTC BP-1-FLAG or FLAG control vector, as described above (Fig. 2). The tumor cells were surgically injected directly into the head of the pancreas of athymic nude mice. The mice injected with DanG and BxPC3 cells were sacrificed 18–20 d and 8 wk after orthotopic injection, respectively. The number of macroscopic metastatic lesions and the volume of the primary tumor were measured upon necropsy. The mice injected with FLAG control cell lines had numerous metastases, primarily on the intestinal wall and in the intestinal mesentery, as well as the liver, diaphragm, and in the abdominal cavity. In marked contrast to the control mice, few tumors were observed outside of the primary tumor in the mice injected with MTCBP-1-FLAG–expressing cell lines (Fig. 6, A and C). Quantification revealed a 92% decrease in metastatic lesions in the mice injected with MTCBP-1–expressing DanG cells compared with controls and a 75% decrease of those injected with BxPC3 cells (Fig. 6, B and D). The volumes of the primary pancreatic tumors were equivalent (Fig. 6, B and D), suggesting that the decreased number of metastases is not an effect on primary tumor formation or growth. Taken together with the in vitro studies described above, these in vivo data provide strong support for MTCBP-1 functioning as an anti-metastatic protein in these tumors.

To confirm that the expression level of MTCBP-1 was maintained in the stable cell lines after injection, we collected both the primary tumor and metastases formed on the intestinal wall from the mice and performed Western blotting for MTCBP-1. As shown in Fig. 6 (E and F), the MTCBP-1-FLAG remained highly expressed in the stable cell lines from both primary tumors. Interestingly, metastatic tumors expressed significantly lower endogenous and ectopically expressed MTCBP-1 than the corresponding primary tumors. These findings suggest that those tumor cells able to metastasize had low or down-regulated levels of MTCBP-1. This further supports a role for MTCBP-1 as a suppressor of invasion and metastasis, where invading cells may express lower levels of the protease-inhibiting MTCBP-1.

As MTCBP-1 reduces metastatic invasion of PDAC via a disruption of MT1-MMP function at invadopodia, we sought to define the expression pattern of these proteins in both human cell lines and tumor tissues. To this end, MT1-MMP and MTCBP-1 levels were compared in nine different human PDAC cell lines by Western blot analysis (Fig. 7 A and Fig. S4 A). Interestingly, MTCBP-1 and MT1-MMP exhibited an inverse expression pattern. DanG, CFPAC, and BxPC3 cells expressed relatively low levels of MTCBP-1 and high levels of MT1-MMP. In contrast, Panc-1, HPAF and HuPT3 cells exhibited high levels of MTCBP-1 and lower levels of MT1-MMP. This inverse expression pattern of MTCBP-1 and MT1-MMP examined in nine different human PDAC cell lines was quantified and shown in Fig. S4 A.

To test if experimental manipulation of MTCBP-1 might lead to a causal increase of MT1-MMP, we treated Panc-1 cells with siRNA to MTCBP-1 and then measured changes in the MT1-MMP levels by Western blotting. As shown in Fig. 7 B, MT1-MMP levels doubled when MTCBP-1 was reduced by siRNA, suggesting that MTCBP-1 may negatively regulate MT1-MMP protein levels. This is also consistent with the Western blots showing MT1-MMP level upon MTCBP-1 depletion in Fig. 1. A similar trend was observed in Panc-1, BxPC3, and DanG cells with an additional siRNA against MTCBP-1 (Fig. S4, B–D).

In addition to changes in total MT1-MMP protein levels, we also tested for changes in protease distribution in MTCBP-1 depleted cells, as an increase or decrease of MT1-MMP on the cell surface could be expected to alter the cells capacity to degrade the surrounding matrix. To test this, Panc-1, BxPC3 and DanG cells were transfected with control siRNAs or siRNAs against MTCBP-1 for 2 d. Cell surface proteins were biotinylated at 4°C for 30 min, and then the cells were lysed and subjected to pulldowns with streptavidin beads. The surface levels of MT1-MMP were tested by Western blotting with antibodies against MT1-MMP (Fig. S4, B–D). Surface MT1-MMP levels were increased following knockdown of MTCBP-1. These findings are consistent with the increased matrix degradation and invadopodia number in the absence of MTCBP-1 and suggest that MTCBP-1 normally restricts MT1-MMP surface expression.

Finally, we tested if increased MT1-MMP levels was a result of transcriptional regulation. To this end, Panc-1, BxPC3, and DanG cells were treated with control siRNAs or MTCBP-1–targeted siRNAs. Quantitative real-time PCR analysis was performed 48 h after transfections. As displayed in Fig. S5, no changes in MT1-MMP mRNA levels were observed upon MTCBP-1 knockdown. This indicates that the regulation of MT1-MMP by MTCBP-1 is post-transcriptional and is likely at the protein level. Collectively, these findings suggest that a combination of increased total MT1-MMP, as well as surface associated MT1-MMP occurs upon the reduction of cellular MTCBP-1. These data are consistent with the inhibitory effects of MTCBP-1 on matrix degradation and in vitro transwell invasion (Fig. 1 and Fig. 2).

To test if the reciprocal expression patterns between MTCBP-1 and MT1-MMP observed in isolated cell lines were also observed in human tumors, tissues from both normal and cancerous regions of 10 PDAC patients were prepared for histological staining of MTCBP-1 and MT1-MMP. As shown in Fig. 7 C, the staining intensity for both MTCBP-1 and MT1-MMP in ductal epithelial cells, stromal cells, and acinar cells from benign tissues appears to be exceptionally modest. In comparison, both MTCBP-1 and MT1-MMP staining was markedly elevated in the cancerous tissues, yet appear to stain distinct cellular populations. MTCBP-1 appears highly expressed in the malignant epithelium but not stroma, while MT1-MMP is the converse, with stronger staining of the surrounding stroma yet modest expression in the ductal tumor cells. Furthermore, the expression level of MTCBP-1 observed in metastatic lesions appears lower than that at the primary tumor site (Fig. 7, C and D), consistent with the decreased expression levels of MTCBP-1 in metastatic versus primary tumors from the orthotopic mouse model described above (Fig. 6, E and F). Interestingly, by analyzing publically available PDAC datasets (Stratford et al., 2010), we found that increased expression of MTCBP-1 is associated with a better overall survival rate among PDAC patients (Figs. 7, E and F), suggesting an important role of MTCBP-1 in PDAC progression. Together, these data support the concept that MTCBP-1 inhibits PDAC invasion and metastasis through binding and inhibition of the pro-invasive protease MT1-MMP.

Discussion

MTCBP-1 as an intrinsic inhibitor of stromal remodeling through a direct interaction with MT1-MMP

Invadopodia are complex yet highly dynamic structures that are precisely controlled during formation and disassembly (Gimona et al., 2008; Poincloux et al., 2009; Ridley, 2011; McNiven, 2013). Here, we have uncovered a novel mechanism regulating invadopodia function in PDAC cells.

We have determined that MTCBP-1 attenuates PDAC cell matrix remodeling and invasion both in vitro and in vivo (Fig. 1, Fig. 2, and Fig. 6). MTCBP-1 has been previously implicated as a negative regulator of MT1-MMP; however, the mechanism and the relevance of this inhibition to cancer remained undefined (Uekita et al., 2004). In this study, we demonstrate that the inhibitory role of MTCBP-1 is dependent on the direct binding of this protein to the CT of MT1-MMP, specifically through residues $PRR^{568–570}$ of MT1-MMP (Fig. 3 and Fig. 4). Deletion of the MTCBP-1 binding site renders MT1-MMP insensitive to the inhibitory effects of MTCBP-1 (Fig. 3 G).

Key to the inhibitory effects of MTCBP-1 is that binding between MTCBP-1 and MT1-MMP disrupts the association between MT1-MMP and F-actin (Fig. 5), which is critical for functional invadopodia (Yu et al., 2012). Studies by others have suggested that F-actin binding captures and concentrates MT1-MMP at the actin-rich invadopodia to promote effective matrix degradation and remodeling during cancer cell invasion (Yu and Machesky, 2012; Yu et al., 2012). The MTCBP-1 binding site on MT1-MMP is directly adjacent to the reported F-actin binding site on MT1-MMP (residues $LLY^{571–573}$), suggesting that MTCBP-1 may displace MT1-MMP from F-actin through competitive binding or steric regulation.

Interestingly, MTCBP-1 is localized at invadopodia, and its overexpression reduces the number of invadopodia in PDAC cells. MTCBP-1 may lead to invadopodia disassembly, or it may prevent the formation of new invadopodia. As MTCBP-1 can disrupt the preestablished association between MT1-MMP and actin (Fig. 5 C), this suggests that MTCBP-1 localization to invadopodia

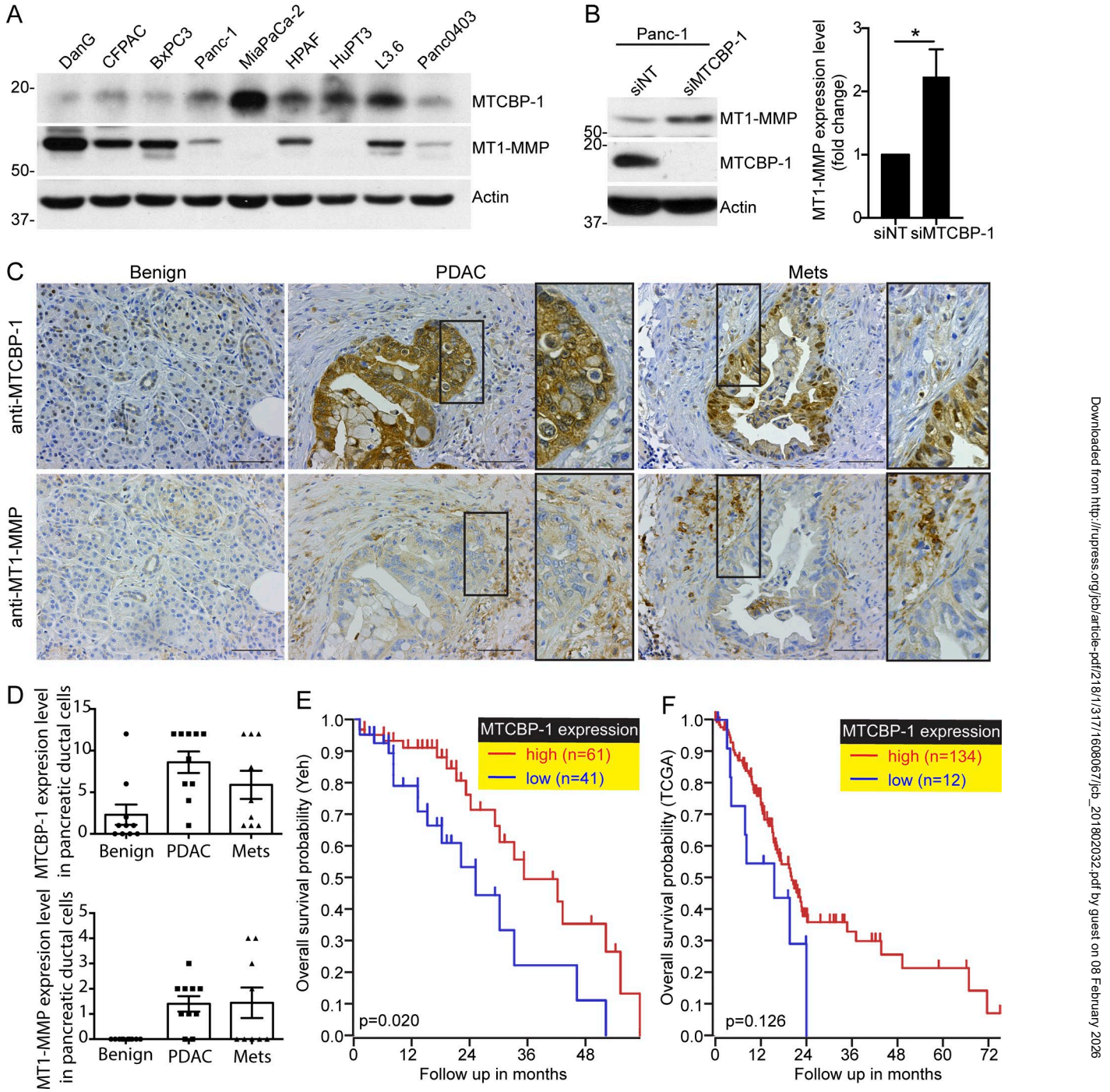

Figure 7. **Differential expression of MTCBP-1 and MT1-MMP in human tumors. (A)** Western blot analysis of MT1-MMP and MTCBP-1 protein levels in nine different PDAC cell lines showing a trend of reciprocal expression. **(B)** Western blot analysis of total MT1-MMP protein level in Panc-1 cells following depletion of MTCBP-1 by siRNA treatment. Quantification shows an increase of MT1-MMP protein level upon MTCBP-1 depletion. Graph represents normalized averages ± SEM from three independent experiments. *, P < 0.05. **(C)** IHC staining of MTCBP-1 and MT1-MMP in serial sections of tissues from pancreatic cancer patients, including normal adjacent pancreas (Benign), PDAC, and metastases from lymph nodes (Mets). Boxed areas are magnified in insets. Bars, 10 µm. **(D)** Semi-quantification of IHC staining of MTCBP-1 and MT1-MMP in pancreatic ductal cells from 10 different patients, showing the expression level of MTC BP-1 and MT1-MMP are increased in primary lesions and metastases. Note that the expression level of MTCBP-1 in metastases is lower than that in the primary tumor. **(E and F)** Kaplan–Meier curves demonstrating the relationship between patient survival and MTCBP-1 expression level in PDAC patients. High MTCBP-1 expression is associated with better overall survival in two cohorts, including the GSE21501 dataset (E) and TCGA dataset (F). All blot measurements in kD.

could induce their disassembly. Thus, MTCBP-1 may also prevent the formation or function of new invadopodia by blocking the capture of MT1-MMP at actin-rich invadopodial precursors. Collectively, MTCBP-1 likely inhibits invadopodia function and tumor cell invasion through disrupting the interaction between MT1-MMP and F-actin.

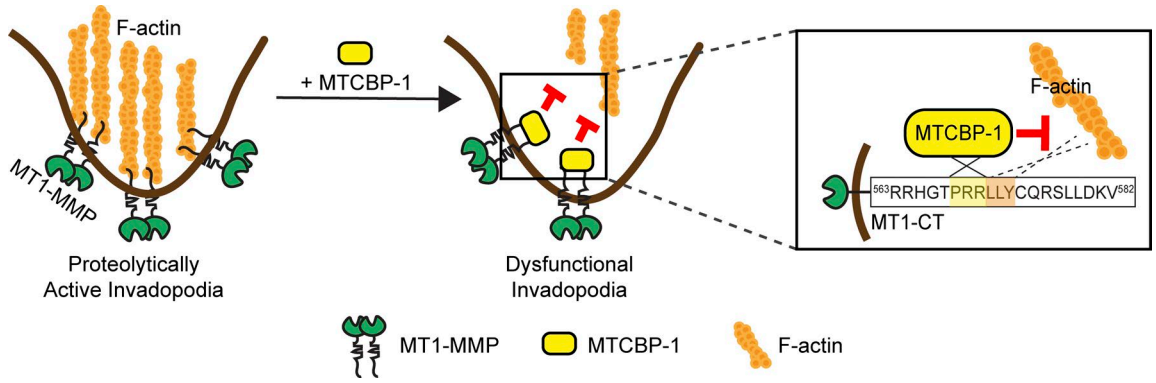

Figure 8. **Proposed model showing functional relationship between MTCBP-1 with MT1-MMP and invadopodia.** In the absence of MTCBP-1, MT1-MMP is sequestered by F-actin at invadopodia to remodel the surrounding stroma through its proteolytic activity. Cells expressing high levels of MTCBP-1 facilitates its binding directly to residues PRR$^{568–570}$ of MT1-MMP and disrupts the association between MT1-MMP and F-actin, which occurs via adjacent residues 571–573 (LLY) on the CT of MT1-MMP. The result of this displacement is a reduction of functional invadopodia and attenuated tumor cell invasion.

Expression of MTCBP-1 is inversely correlated with MT1-MMP expression and reduces tumor metastasis

MT1-MMP that is unable to bind to F-actin and is not sequestered at invadopodia is trafficked back into the cell via endosomal trafficking (Yu et al., 2012). Thus, it is likely that a cellular protein such as MTCBP-1 that interferes with this interaction is likely to alter protease distribution. The biochemical studies displayed in Fig. 5 (C–F) using two distinct methods indicate that MTCBP-1 disrupts the interaction between MT1-MMP and F-actin. Thus, we predict that MTCBP-1 could facilitate the clearance of MT1-MMP from invadopodia via an endosomal compartment. This may occur through lateral movement of MT1-MMP to a different region of plasma membrane or through the endocytosis of MT1-MMP into the cell (Ballestrem et al., 2001; Jiang et al., 2001; Ludwig et al., 2008; El Azzouzi et al., 2016). It is known that MT1-MMP can be cleared from the plasma membrane through endocytosis and trafficking to the endosomes and can then be degraded by lysosomes or recycled back to the plasma membrane (Jiang et al., 2001; Ludwig et al., 2008; Poincloux et al., 2009; Eisenach et al., 2012). As MTCBP-1 disturbs the interaction between MT1-MMP and F-actin, which is important for the sequestration of MT1-MMP at invadopodia; this may cause the clearance of MT1-MMP and subsequent down-regulation of MT1-MMP through lysosomal-mediated degradation. Consistent with this concept, our data suggest that MTCBP-1 negatively regulates MT1-MMP protein level, as RNAi-mediated knockdown of MTCBP-1 resulted in a twofold increase in MT1-MMP protein level (Fig. 7 B). In addition, we observed an inverse correlation in a subset of cultured PDAC cells (Fig. 7 A). These changes in protease levels were not due to increased transcriptional activity (Fig. S5) but perhaps an increased association with the cell surface (Fig. S4, B–D), thus increasing protease access to the stromal substrate. However, experimentally increasing the expression of MTCBP-1 in cells in culture (Fig. 2, A–C) or injected into mice (Fig. 6, E and F) did not alter MT1-MMP expression, as we might have predicted based on the spontaneous expression levels observed in cultured PDAC cells (Fig. 2, A–C). Why these overexpression studies did not show a decrease in protease levels is unclear, but suggests that additional factors might be required to regulate MT1-MMP.

MTCBP-1 expression level in primary lesions and metastases

Based on the anti-invasive role of MTCBP-1, we predicted that its expression may be down-regulated in tumor cells. Unexpectedly, we observed that MTCBP-1 protein levels are, in fact, elevated in human pancreatic tumors compared with control pancreas, which paradoxically suggested that metastatic invasion may be suppressed in these MTCBP-1–expressing tumor cells. Strikingly, while MTCBP-1 was elevated in primary tumors, we found that MTCBP-1 protein levels were decreased in metastatic lesions compared with the primary tumor. This differential expression was observed in both human tumor samples and in orthotopic mouse models (Figs. 6, E and F; and Fig. 7 C) and suggests that down-regulation of MTCBP-1 may contribute to metastasis in vivo. These reductions in MTCBP-1 protein levels in metastatic lesions are consistent with previous findings showing a decrease in the expression of this protein correlates with an increasing in the grade of brain tumors (Pratt et al., 2016). Metastatic invasion may result from a suppression of MTCBP-1 expression, or metastases may be derived from a subset of cancer cells that express relatively low levels of MTCBP-1. As described above, MTCBP-1 may negatively regulate the protein levels of the pro-invasive protease MT1-MMP in cell lines. Physiologically, this supports the concept that a subset of PDAC cells is highly invasive and primed for metastatic dissemination, specifically those with decreased MTCBP-1, and this subpopulation might contribute to the high metastatic rate and low survival rate of patients and be a prime target for novel therapies for PDAC patients (Fig. 8).

In addition to binding to MT1-MMP, MTCBP-1 also functions in the methionine salvage pathway where it can produce the precursor of methionine (Hirano et al., 2005). Intriguingly, methionine dependency has been observed in different types of cancer (Dumontet et al., 1996; Cavuoto and Fenech, 2012). Collectively, this study establishes MTCBP-1 as a novel invadopodial protein that functions as a specific endogenous inhibitor of MT1-MMP, inhibits MT1-MMP–mediated matrix remodeling, and thus invasion and metastasis, through disrupting the binding between MT1-MMP and F- actin.

Materials and methods

Cell culture

DanG, Panc-1, MiaPaCa-2, CFPAC, HuPT3, and HPAF-II human PDAC cells were maintained in DMEM containing 10% FBS. BxPC3, Panc0403, and L3.6 were maintained in RPMI-1640 containing 10% FBS. All cells were grown in a 5% CO_2, 95% air incubator at 37°C. The cell lines are obtained from ATCC or were gifts from D. Billadeau (Mayo Clinic, Rochester, MN) or M. Fernandez-Zapico (Mayo Clinic).

Stable cell lines

MTCBP-1 was cloned into the pLenti6.3.FLAG lentiviral vector (D. Billadeau) and was cotransfected into HEK 293T cells at 70% confluency with the third generation packaging plasmid obtained from Y. Ikeda (Mayo Clinic). The pLenti6.3.FLAG vector was used as a control. Viral supernatants were collected after 72 h, centrifuged, and filtered through 0.45-µm filters. To obtain stable expression of FLAG or MTCBP-1-FLAG, semi-confluent DanG, BxPC3, and Panc-1 cells were transduced with viral particles with 10 µg/ml polybrene. 3 d after transduction, cells were shifted to culture medium containing 5 µg/ml Blasticidin for 2 wk for selection.

Plasmid and siRNA transfections

MT1-MMP-mCherry construct were gifts from P. Chavrier (Institut Curie, Paris, France). MT1-MMP-ΔPRR-mCherry was generated from mutagenesis based on the MT1-MMP-mCherry construct. Tks5 was cloned from the pECE M2-SH3PXD2A WT construct (Addgene) and inserted into the pEGFP-C1 construct (Addgene). The MT1-CT-GST construct and all its related mutants used in this study were generated with annealing oligonucleotides integrated into the pGEX-4T-1 construct (Addgene). ACTN-N was cloned from a HeLa cDNA library and inserted into the pGEX-4T-1 vector. The His-MTCBP-1 construct was generated by amplifying MTCBP-1 from a HeLa cDNA library and inserted into the pQE-80L vector (Invitrogen). Lipofectamine 2000 (Invitrogen) was used for plasmid transfection according to the manufacturer's protocol. Lipofectamine RNAi Max (Invitrogen) was used for siRNA transfection according to the manufacturer's protocol. Nontargeting siRNA and all targeting siRNAs were from Dharmacon (Thermo Fisher Scientific): human MMP-14 (siMT1-MMP; no. D-004145-02-0010) and MTCBP-1 (siMTCBP-1; no. J-020394-10-0010; siMTCBP-1-2; no. J-0200394-11-0010).

Immunoblotting

To analyze protein levels, cells were lysed in NP-40 lysis buffer (20 mM Tris-Cl, pH 8.0, 137 mM NaCl, 10% glycerol, 1% NP-40, and 2 mM EDTA) containing complete protease inhibitors (Roche) with sonication. To analyze protein levels in mouse tumor samples, tissues were lysed in radio-IP assay (RIPA) buffer (50 mM Tris, pH 8.0, 150 mM NaCl, 1% NP-40, 0.5% deoxycholate, 0.1% SDS, 2 mM Na_3VO_4, and 15 mM NaF) containing complete protease inhibitors (Roche) with dounce homogenizers. The protein concentrations were determined by BCA assay (Pierce), and equal amount of proteins were resolved by SDS-PAGE through electrophoresis and transferred to PVDF membranes for antibody probing. The primary antibodies used were MTCBP-1 (designed against peptide YMDDAPGDPRQPHRPDPGRPVG, developed by Covance and purified in the laboratory as described previously; McNiven et al., 2000), MT1-MMP (Abcam), Actin (Sigma), GST (Santa Cruz), and GFP (Santa Cruz). The secondary antibodies were horseradish peroxidase–conjugated and purchased from Biosource International. Immunoreactive signals were detected with SuperSignal West Pico Chemiluminescent substrate (Thermo Fisher Scientific) and exposed to autoradiographic films (HyBlot CL).

Co-IP and GST pulldown

Equal number of cells were seeded in culture medium on 10-cm plates until 90% confluency and collected by scraping cells into 1ml of lysis buffer (NP-40 lysis buffer for co-IP, and TEN100 [20 mM Tris, pH 7.4, 0.1 mM EDTA, and 100 mM NaCl] containing complete protease inhibitors [Roche] for GST pulldown). Cell debris was removed by centrifugation. The concentration of the proteins in the supernatant was determined by BCA assay (Pierce).

For co-IP, the supernatants were precleared for 30 min with Protein A sepharose (Sigma) for MTCBP-1 co-IP experiments, or Protein G beads for actin co-IP experiments (Abcam), before IP with appropriate antibodies and beads. Samples were washed with NP-40 lysis buffer (high salt; 20 mM Tris-Cl, pH 8.0, 150 mM NaCl, 10% glycerol, 1% NP-40, and 2 mM EDTA) containing complete protease inhibitors (Roche) and resolved by SDS-PAGE gel and immunoblotted as described above.

For GST pulldowns, the supernatants were incubated with purified GST or GST fusion protein expressed in and purified from *Escherichia coli* BL21 cells using Glutathione Sepharose 4B (GE Healthcare) according to the manufacturer's protocol. Similarly, for GST pulldowns with His-MTCBP-1 (purified with Ni_2-coated beads [Roche] based on the manufacturer's protocol), His-MTC BP-1 was incubated with GST proteins in TEN100 buffer for 1 h. The beads were washed with NTEN300 buffer (20 mM Tris, pH 7.4, 0.1 mM EDTA, 300 mM NaCl, and 0.05% NP-40) containing complete protease inhibitors (Roche) and resolved by SDS-PAGE and immunoblotted.

Actin co-sedimentation assay

G-actin (rabbit skeletal muscle actin protein, >99% pure; Cytoskeleton, Inc.) was prepared according to the manufacturer's protocol with G buffer (2 mM Tris, pH 8.0, 0.2 mM $CaCl_2$, 0.2 mM ATP, 0.5 mM DTT). All purified proteins including GST, GST-MT1-MMP-CT, and HIS-MTCBP-1 were dialyzed in G buffer after purification and subjected to centrifugation (100,000 *g* for 20 min at 4°C) to remove insoluble proteins. The indicated amount of purified proteins and G-actin were added into each individual reaction in a total volume of 200 µl that was equilibrated with G buffer. Subsequently, 20 µl of F buffer (20 mM Tris, pH 7.5, 2 mM $CaCl_2$, 1 M KCl, 20 mM $MgCl_2$, 10 mM ATP, and 5 mM DTT) was added to each reaction and incubated for 1 h before pelleting (100,000 *g* for 1 h at 25°C) in a Beckman table-top centrifuge. Pellets and supernatants were separated and brought up to equal volume and 40 µl of the samples were resolved by SDS-PAGE gels and immunoblotted.

Biotinylation assay

Equal number of cells were seeded in culture medium on 10-cm plates and treated with control siRNAs or siRNAs against MTCBP-1 for 2 d. The cells were then transferred to 4°C, washed with ice-cold PBS, incubated with 0.5 mg/ml biotin (EZ-link Sulfo-NHS-LC Biotin; Thermo Fisher Scientific) for 30 min, followed by 50 mM NH_4Cl to quench biotin. Subsequently, cells were rinsed with ice-cold PBS for three times, lysed with RIPA buffer (50 mM Tris, pH 8.0, 150 mM NaCl, 1% NP-40, 0.5% deoxycholate, 0.1% SDS, 2 mM Na_3VO_4, and 15 mM NaF), and sonicated. Cell debris was removed by centrifugation for 10 min at 14,000 rpm and 4°C. Equal amounts of protein from individual samples were incubated with 50 µl of streptavidin-agarose beads (Thermo Fisher Scientific) according to the manufacturer's protocol, washed three times in RIPA buffer, and subjected to Western blot analysis using the anti–MT1-MMP antibody.

Far-Western blotting assays

Far-Western blotting was performed as described previously (Wang et al., 2011). Equal amounts of purified GST and GST fusion proteins were resolved by SDS-PAGE and transferred to PVDF membranes. Then the membranes were blocked in basic buffer (20 mM Hepes, pH 7.5, 50 mM KCl, 10 mM $MgCl_2$, 1 mM dithiothreitol, and 0.1% Igepal CA-630) containing 10% nonfat dry milk overnight at 4°C and then incubated in interaction buffer (basic buffer with 1.5% nonfat dry milk) containing 2 µg/ml of purified His-MTCBP-1 protein or 4 µM of F-actin for 1 h at room temperature. The F-actin was polymerized from G-actin (Cytoskeleton, Inc.) based on the manufacturer's protocol. The membranes were washed three times with PBS-T and probed with antibodies to MTCBP-1, His epitope tag (Cell Signaling), or actin. The membrane was then stripped and probed with GST to confirm equal loading of the GST proteins. For experiments testing if MTCBP-1 disrupts the preestablished interaction between GST fusion proteins and F-actin, the membranes containing GST fusion proteins were incubated with interaction buffer containing 0.35 µM MTCBP-1 or not for 2 h at room temperature, following the actin incubation. The subsequent steps were similar to the standard far-Western blotting assays.

Immunofluorescence

Cells were fixed and prepared for immunofluorescence as described previously (Wang et al., 2011). Coverslips were incubated in primary antibodies for 2 h at 37°C. The primary antibodies used were FLAG (Cell Signaling), MT1-MMP (Abcam), and Tks5 (Santa Cruz). Then the coverslips were washed with D-PBS and incubated in labeled secondary antibodies (Life Technologies) for 1 h at room temperature. Actin was visualized by TRITC-phalloidin or Phalloidin-Atto 390 (Sigma Aldrich) staining. Prolong mounting medium (Life Technologies) was used to mount the coverslips before imaging. Fluorescence images were acquired using epifluorescence microscopes (Axio Observer and Axiovert 200; Carl Zeiss MicroImaging) using a 63× oil objective, unless otherwise indicated, with iVision software. For confocal microscopy, cells were imaged with a Zeiss LSM 780 confocal microscope (Carl Zeiss MicroImaging) and a 63×/1.2-NA water immersion lens. Images were processed and adjusted with Adobe Photoshop software (Adobe) uniformly to the entire image.

Time-lapse microscopy

BxPC3 cells stably expressing FLAG or MTCBP-1-FLAG transfected with Tks5-GFP, as described above, were plated on clear gelatin-coated, glass-bottomed imaging dishes (MatTek Corporation). The cells were then imaged using an Axio Observer.Z1/7 microscope (Carl Zeiss MicroImaging) with a 63× water lens (NA 1.2) with stage top incubation set at 37°C and 5% CO_2. Images were acquired every 5 min for 200 frames (16 h and 40 min elapsed time). Movies were converted from 480 × 320-pixel Zen image sequences using MPEG encoding.

Matrix degradation assays

Gelatin-coated coverslips were prepared as described in the presence or absence of Oregon green–conjugated gelatin (Invitrogen), diluted in 0.2% gelatin (Sigma Aldrich; Wang and McNiven, 2012). Cells were first transfected with the indicated constructs for 1 d or siRNAs for 2 d, then replated onto gelatin-coated coverslips in the presence of the MMP inhibitor BB94 overnight (5 µM; Millipore), and then rinsed at least three times with HBSS and culture medium to provide a synchronized starting point for cell-based gelatin degradation over the indicated time before fixation. The cell border represented by actin staining was visualized by TRITC-phalloidin or Phalloidin-Atto 390 (Sigma Aldrich) and viewed by immunofluorescence. The percentage of cells that degraded the gelatin matrix was scored with ≥100 cells that were randomly imaged. The degradation area of the cells degrading matrix was quantified and normalized to the total cell area with ImageJ software (Martin et al., 2012).

Transwell assays

3×10^5 cells were seeded in 6-well transwell chambers containing 8-µm diameter pores (Millipore) that were coated with 0.3% gelatin substrate before the seeding of cells. Invasion was promoted by establishing a 10% to 0.1% serum gradient from the bottom to the top of the transwell, respectively, over 6 h for BxPC3 cells, 24 h for Panc-1 cells, and 48 h for DanG cells. Cell invasion was measured as the number of DAPI (Abcam)–positive nuclei at the top versus the bottom of the membrane over time.

Orthotopic mouse studies

All animal experiments were performed under Institutional Animal Care and Use Committee approval and in accordance with the approved protocol. Athymic nu/nu mice (4–6 wk old) were purchased from Jackson Laboratory. Mice were anesthetized by intraperitoneal injection of ketamine and xylazine before the surgery. 10^6 BxPC3 or DanG cells stably expressing FLAG or MTCBP-1-FLAG were resuspended in 100 µl PBS and orthotopically implanted into the head of the pancreas. Mice were weighed every other day to check health conditions. At 18–20 d (DanG) or 8 wk (BxPC3) or upon a weight loss of >20% body weight, mice were sacrificed and both macroscopic metastatic tumors and primary tumors were analyzed upon necropsy.

Immunohistochemistry (IHC)

30 different histological samples from 10 de-identified patients were obtained from the Mayo Clinic SPORE in Pancreatic Cancer tissue core. All patients provided informed consent and all studies were conducted with the approval of the Institutional Review Board. The three tissue samples from each patient were benign, PDAC and tissue from a site of metastasis. The serial sections of the tissues were stained with MT1-MMP (Abcam) and MTC BP-1 (Proteintech) antibodies by the Pathology Research Core (Mayo Clinic). Numerical scoring of stained tissue intensity was semi-quantitative and performed by a pathologist (L. Zhang) with respect to intensity (scale: 0–3) and extent (scale: 0–4) in the Mayo Clinic Department of Anatomical Pathology.

Quantification and statistical analysis

Statistical analysis was conducted using GraphPad Prism. Graphed data represent the mean ± SEM of at least three independent experiments. The Student's *t* test was used to determine the statistical significance. A P value lower than 0.05 represented a statistically significant difference.

Online supplemental material

Fig. S1 shows MTCBP-1 inhibits the invasive properties of PDAC cells through MT1-MMP (related to Fig. 1). Fig. S2 shows MTC BP-1 expression alters invadopodia dynamics (related to Figs. 1–3). Fig. S3 shows MTCBP-1 prevents the retention of MT1-MMP at invadopodia (related to Fig. 4). Fig. S4 shows that MTC BP-1 regulates both the total and the cell surface MT1-MMP protein levels in PDAC cells (related to Fig. 1 and Fig. 7). Fig. S5 shows MTCBP-1 does not regulate MT1-MMP transcription (related to Fig. 1, Fig. 7, and Fig. S4). Videos 1 and 2 show that invadopodia are more transient in cells expressing increased levels of MTCBP-1.

Acknowledgments

We thank Dr. Philippe Chavrier (Institut Curie, Paris, France) for providing the MT1-MMP-mCherry construct, Dr. Daniel Billadeau (Mayo Clinic, Rochester, MN) for the pLenti6.3.F-MCS vector, and members of the McNiven Laboratory, especially Zhipeng Li for helpful discussions and input.

This work was supported by the National Institutes of Health National Cancer Institute grant R01 CA104125 (to M.A. McNiven and G.L. Razidlo), the Mayo Clinic Center for Cell Signaling in Gastroenterology (grant NIDDK P30DK084567), the Mayo Clinic SPORE in Pancreatic Cancer (P50 CA102701), and the Mayo Clinic Sydney Luckman Family Predoctoral Fellowship (to L. Qiang).

The authors declare no competing financial interests.

Author contributions: L. Qiang, H. Cao, and J. Chen performed most of the experiments, and L. Qiang and S.G. Weller carried out the in vivo studies. E.W. Kruger performed live-cell imaging and related quantification. L. Zhang analyzed and scored the IHC staining. L. Qiang, H. Cao, and M.A. McNiven designed the work and analyzed the data. L. Qiang, G.L. Razidlo, and M.A. McNiven wrote and revised the manuscript.

Submitted: 7 February 2018
Revised: 28 September 2018
Accepted: 29 October 2018

References

American Cancer Society. 2015. Cancer Facts & Figures 2015. American Cancer Society, Atlanta.

American Cancer Society. 2017. Cancer Facts & Figures 2017. American Cancer Society, Atlanta.

Artym, V.V., Y. Zhang, F. Seillier-Moiseiwitsch, K.M. Yamada, and S.C. Mueller. 2006. Dynamic interactions of cortactin and membrane type 1 matrix metalloproteinase at invadopodia: defining the stages of invadopodia formation and function. *Cancer Res.* 66:3034–3043. https://doi.org/10.1158/0008-5472.CAN-05-2177

Ballestrem, C., B. Hinz, B.A. Imhof, and B. Wehrle-Haller. 2001. Marching at the front and dragging behind: differential alphaVbeta3-integrin turnover regulates focal adhesion behavior. *J. Cell Biol.* 155:1319–1332. https://doi.org/10.1083/jcb.200107107

Cavuoto, P., and M.F. Fenech. 2012. A review of methionine dependency and the role of methionine restriction in cancer growth control and life-span extension. *Cancer Treat. Rev.* 38:726–736. https://doi.org/10.1016/j.ctrv.2012.01.004

Chan, K.T., C.L. Cortesio, and A. Huttenlocher. 2009. FAK alters invadopodia and focal adhesion composition and dynamics to regulate breast cancer invasion. *J. Cell Biol.* 185:357–370. https://doi.org/10.1083/jcb.200809110

Clark, E.S., A.S. Whigham, W.G. Yarbrough, and A.M. Weaver. 2007. Cortactin is an essential regulator of matrix metalloproteinase secretion and extracellular matrix degradation in invadopodia. *Cancer Res.* 67:4227–4235. https://doi.org/10.1158/0008-5472.CAN-06-3928

Dumontet, C., A.M. Roch, and G. Quash. 1996. Methionine dependence of tumor cells: programmed cell survival? *Oncol. Res.* 8:469–471.

Eddy, R.J., M.D. Weidmann, V.P. Sharma, and J.S. Condeelis. 2017. Tumor Cell Invadopodia: Invasive Protrusions that Orchestrate Metastasis. *Trends Cell Biol.* 27:595–607. https://doi.org/10.1016/j.tcb.2017.03.003

Egeblad, M., and Z. Werb. 2002. New functions for the matrix metalloproteinases in cancer progression. *Nat. Rev. Cancer.* 2:161–174. https://doi.org/10.1038/nrc745

Eisenach, P.A., P.C. de Sampaio, G. Murphy, and C. Roghi. 2012. Membrane type 1 matrix metalloproteinase (MT1-MMP) ubiquitination at Lys581 increases cellular invasion through type I collagen. *J. Biol. Chem.* 287:11533–11545. https://doi.org/10.1074/jbc.M111.306340

El Azzouzi, K., C. Wiesner, and S. Linder. 2016. Metalloproteinase MT1-MMP islets act as memory devices for podosome reemergence. *J. Cell Biol.* 213:109–125. https://doi.org/10.1083/jcb.201510043

Gimona, M., R. Buccione, S.A. Courtneidge, and S. Linder. 2008. Assembly and biological role of podosomes and invadopodia. *Curr. Opin. Cell Biol.* 20:235–241. https://doi.org/10.1016/j.ceb.2008.01.005

Hirano, W., I. Gotoh, T. Uekita, and M. Seiki. 2005. Membrane-type 1 matrix metalloproteinase cytoplasmic tail binding protein-1 (MTCBP-1) acts as an eukaryotic aci-reductone dioxygenase (ARD) in the methionine salvage pathway. *Genes Cells.* 10:565–574. https://doi.org/10.1111/j.1365-2443.2005.00859.x

Jacob, A., and R. Prekeris. 2015. The regulation of MMP targeting to invadopodia during cancer metastasis. *Front. Cell Dev. Biol.* 3:4. https://doi.org/10.3389/fcell.2015.00004

Jiang, A., K. Lehti, X. Wang, S.J. Weiss, J. Keski-Oja, and D. Pei. 2001. Regulation of membrane-type matrix metalloproteinase 1 activity by dynamin-mediated endocytosis. *Proc. Natl. Acad. Sci. USA.* 98:13693–13698. https://doi.org/10.1073/pnas.241293698

Linder, S. 2007. The matrix corroded: podosomes and invadopodia in extracellular matrix degradation. *Trends Cell Biol.* 17:107–117. https://doi.org/10.1016/j.tcb.2007.01.002

Ludwig, T., S.M. Theissen, M.J. Morton, and M.J. Caplan. 2008. The cytoplasmic tail dileucine motif LL572 determines the glycosylation pattern of membrane-type 1 matrix metalloproteinase. *J. Biol. Chem.* 283:35410–35418. https://doi.org/10.1074/jbc.M801816200

Martin, K.H., K.E. Hayes, E.L. Walk, A.G. Ammer, S.M. Markwell, and S.A. Weed. 2012. Quantitative measurement of invadopodia-mediated extracellular matrix proteolysis in single and multicellular contexts. *J. Vis. Exp.* (66):e4119.

McNiven, M.A. 2013. Breaking away: matrix remodeling from the leading edge. *Trends Cell Biol.* 23:16–21. https://doi.org/10.1016/j.tcb.2012.08.009

McNiven, M.A., L. Kim, E.W. Krueger, J.D. Orth, H. Cao, and T.W. Wong. 2000. Regulated interactions between dynamin and the actin-binding protein cortactin modulate cell shape. *J. Cell Biol.* 151:187–198. https://doi.org/10.1083/jcb.151.1.187

Murphy, D.A., and S.A. Courtneidge. 2011. The 'ins' and 'outs' of podosomes and invadopodia: characteristics, formation and function. *Nat. Rev. Mol. Cell Biol.* 12:413–426. https://doi.org/10.1038/nrm3141

Pahwa, S., M.J. Stawikowski, and G.B. Fields. 2014. Monitoring and Inhibiting MT1-MMP during Cancer Initiation and Progression. *Cancers (Basel).* 6:416–435. https://doi.org/10.3390/cancers6010416

Paterson, E.K., and S.A. Courtneidge. 2018. Invadosomes are coming: new insights into function and disease relevance. *FEBS J.* 285:8–27. https://doi.org/10.1111/febs.14123

Poincloux, R., F. Lizárraga, and P. Chavrier. 2009. Matrix invasion by tumour cells: a focus on MT1-MMP trafficking to invadopodia. *J. Cell Sci.* 122:3015–3024. https://doi.org/10.1242/jcs.034561

Pratt, J., M. Iddir, S. Bourgault, and B. Annabi. 2016. Evidence of MTCBP-1 interaction with the cytoplasmic domain of MT1-MMP: Implications in the autophagy cell index of high-grade glioblastoma. *Mol. Carcinog.* 55:148–160. https://doi.org/10.1002/mc.22264

Rahib, L., B.D. Smith, R. Aizenberg, A.B. Rosenzweig, J.M. Fleshman, and L.M. Matrisian. 2014. Projecting cancer incidence and deaths to 2030: the unexpected burden of thyroid, liver, and pancreas cancers in the United States. *Cancer Res.* 74:2913–2921. https://doi.org/10.1158/0008-5472.CAN-14-0155

Rakash, S. 2012. Role of proteases in cancer: A review. *Biotechnology and Molecular Biology Reviews.* 7:90–101. https://doi.org/10.5897/BMBR11.027

Ridley, A.J. 2011. Life at the leading edge. *Cell.* 145:1012–1022. https://doi.org/10.1016/j.cell.2011.06.010

Sabeh, F., R. Shimizu-Hirota, and S.J. Weiss. 2009. Protease-dependent versus -independent cancer cell invasion programs: three-dimensional amoeboid movement revisited. *J. Cell Biol.* 185:11–19. https://doi.org/10.1083/jcb.200807195

Siegel, R.L., K.D. Miller, and A. Jemal. 2016. Cancer statistics, 2016. *CA Cancer J. Clin.* 66:7–30. https://doi.org/10.3322/caac.21332

Siegel, R.L., K.D. Miller, and A. Jemal. 2017. Cancer Statistics, 2017. *CA Cancer J. Clin.* 67:7–30. https://doi.org/10.3322/caac.21387

Stratford, J.K., D.J. Bentrem, J.M. Anderson, C. Fan, K.A. Volmar, J.S. Marron, E.D. Routh, L.S. Caskey, J.C. Samuel, C.J. Der, et al. 2010. A six-gene signature predicts survival of patients with localized pancreatic ductal adenocarcinoma. *PLoS Med.* 7:e1000307. https://doi.org/10.1371/journal.pmed.1000307

Uekita, T., I. Gotoh, T. Kinoshita, Y. Itoh, H. Sato, T. Shiomi, Y. Okada, and M. Seiki. 2004. Membrane-type 1 matrix metalloproteinase cytoplasmic tail-binding protein-1 is a new member of the Cupin superfamily. A possible multifunctional protein acting as an invasion suppressor down-regulated in tumors. *J. Biol. Chem.* 279:12734–12743. https://doi.org/10.1074/jbc.M309957200

Wang, Y., and M.A. McNiven. 2012. Invasive matrix degradation at focal adhesions occurs via protease recruitment by a FAK-p130Cas complex. *J. Cell Biol.* 196:375–385. https://doi.org/10.1083/jcb.201105153

Wang, Y., H. Cao, J. Chen, and M.A. McNiven. 2011. A direct interaction between the large GTPase dynamin-2 and FAK regulates focal adhesion dynamics in response to active Src. *Mol. Biol. Cell.* 22:1529–1538. https://doi.org/10.1091/mbc.e10-09-0785

Yu, X., and L.M. Machesky. 2012. Cells assemble invadopodia-like structures and invade into matrigel in a matrix metalloprotease dependent manner in the circular invasion assay. *PLoS One.* 7:e30605. https://doi.org/10.1371/journal.pone.0030605

Yu, X., T. Zech, L. McDonald, E.G. Gonzalez, A. Li, I. Macpherson, J.P. Schwarz, H. Spence, K. Futó, P. Timpson, et al. 2012. N-WASP coordinates the delivery and F-actin-mediated capture of MT1-MMP at invasive pseudopods. *J. Cell Biol.* 199:527–544. https://doi.org/10.1083/jcb.201203025